



Cite This: J. Phys. Chem. C 2019. 123. 24328–24337

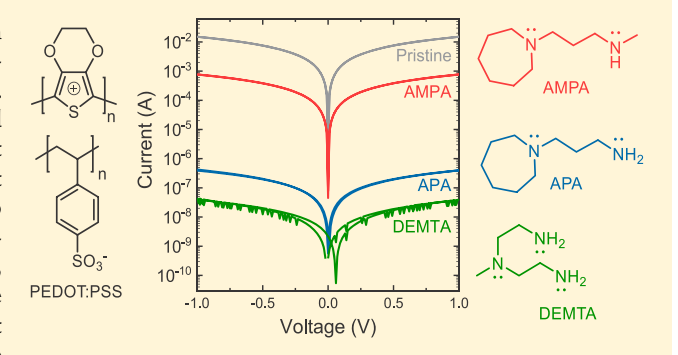
pubs.acs.org/JPCC

The Mechanism of Dedoping PEDOT:PSS by Aliphatic Polyamines

Tom P. A. van der Pol,[†] Scott T. Keene,^{§©} Bart W. H. Saes,[†] Stefan C. J. Meskers,^{†©} Alberto Salleo,[§] Yoeri van de Burgt,**,‡® and René A. J. Janssen*,†®

Supporting Information

ABSTRACT: Poly(3,4-ethylenedioxythiophene) blended with polystyrenesulfonate and poly(styrenesulfonic acid), PE-DOT:PSS, has found widespread use in organic electronics. Although PEDOT:PSS is commonly used in its doped electrically conducting state, the ability to efficiently convert PEDOT:PSS to its undoped nonconducting state is of interest for a wide variety of applications ranging from biosensors to organic neuromorphic devices. Exposure to aliphatic monoamines, acting as an electron donor and Brønsted-Lowry base, has been reported to be partly successful, but monoamines are unable to fully dedope PEDOT:PSS. Remarkably, some—but not all—polyamines can dedope PEDOT:PSS very efficiently to



very low conductivity levels, but the exact chemical mechanism involved is not understood. Here, we study the dedoping efficacy of 21 different aliphatic amines. We identify the presence of two or more primary amines, which can participate in an intramolecular reaction, as the key structural motif that endows polyamines with high PEDOT:PSS dedoping strength. A multistep reaction mechanism, involving sequential electron transfer and deprotonation steps, is proposed that consistently explains the experimental results. Finally, we provide a simple method to convert the commonly used aqueous PEDOT:PSS dispersion into a precursor formulation that forms fully dedoped PEDOT:PSS films after spin coating and subsequent thermal annealing.

■ INTRODUCTION

The blend of poly(3,4-ethylenedioxythiophene) and polystyrenesulfonate (PEDOT:PSS) is the most widely used conducting polymer in organic electronic devices and has been extensively used in a wide variety of applications such as organic light-emitting diodes, solar cells, thermoelectric devices, batteries, supercapacitors, and fuel cells.¹⁻⁴ Unlike most semiconducting polymers, PEDOT:PSS is synthesized in a doped (i.e., conducting) state. The partially oxidized (doped) PEDOT chains are charge-compensated by deprotonated sulfonic acid groups of PSS. PEDOT:PSS has excellent filmforming properties, is relatively stable under ambient conditions, is transparent in the visible region, and features tunable conductivity and work function. PEDOT:PSS is commercially available as a dispersion in water at low pH and can be used to form highly conductive polymeric thin films in combination with cosolvents.5

Recently, a growing research interest is devoted to the application of semiconducting polymers in a variety of biosensors, commonly using organic electrochemical transistors (OECTs), which are utilized to monitor and control biological processes. In particular, organic electronic materials have emerged as the preferred platform because of their

biocompatibility and "soft" nature. 6,7 PEDOT:PSS has become a popular choice as the transducing material, primarily because of excellent ionic and electronic conduction when interfacing with aqueous electrolytes. 8,9 This results in a bulk modulation of conductivity and endows the material with high transconductance and low operating voltages when used as the channel material. However, devices based on PEDOT:PSS typically operate in depletion mode because of its intrinsically doped (conducting) state. In this mode the conductivity is reduced upon application of gate bias. Instead, operation in accumulation mode would be more favorable as it lowers energy consumption (i.e., virtually no current flows) in the "off" state. Naturally, accumulation mode operation requires an intrinsic (undoped) semiconductor as active material. Devices operating in accumulation mode have been demonstrated by using specifically synthesized intrinsic materials, 10 but the synthesis of these organic semiconductors is complex, timeconsuming, and costly. Ideally, one would be able to use PEDOT:PSS in accumulation mode, combining low-energy

Received: August 13, 2019 Revised: September 6, 2019 Published: September 6, 2019



[†]Department of Chemical Engineering and Chemistry and Institute for Complex Molecular Systems and [‡]Department of Mechanical Engineering and Institute for Complex Molecular Systems, Eindhoven University of Technology, 5600 MB Eindhoven, The Netherlands

[§]Department of Materials Science and Engineering, Stanford University, Stanford, California 94305, United States

Table 1. Electrical $(R_{\rm E})$ and Optical $(R_{\rm O})$ Ratio of Dedoping PEDOT:PSS with Organic Amines^a

Compound	Acronym	Structural formula	$R_{ m E}$	$R_{\rm O}$
<i>n</i> -butylamine	n-BA	NH_2	1.6×10^{1}	2.02
<i>N,N,N',N'</i> -tetramethyl-1,2-ethanediamine	TeMEDA		5.5×10^2	5.13
<i>N,N,N'</i> -trimethyl-1,2-ethanediamine	TrMEDA	, NH H	4.7×10^{2}	2.99
<i>N,N</i> -dimethyl-1,2-thanediamine	1,1- DMEDA	N N NH ₂	3.7×10^{2}	4.14
<i>N,N'</i> -dimethyl-1,2-thanediamine	1,2- DMEDA	;;	1.4×10^4	5.87
<i>N</i> -methyl-1,2-ethanediamine	MEDA	NH2	3.2×10^{6}	7.78
1,2-ethanediamine	EDA	H ₂ N NH ₂	1.1×10^{6}	27.4
1,5-pentanediamine	Cadaverine	NH ₂	3.1×10^{6}	7.32
<i>N</i> -(2-aminoethyl)-1,2-ethanediamine	DETA	NH_2 NH_2 NH_2 NH_2	5.9 × 10 ⁶	25.4
<i>N</i> -(2-aminoethyl)- <i>N</i> -methyl-1,2-ethanediamine	DEMTA	NH_2 NH_2 NH_2 NH_2	1.8×10^{5}	33.8
cis-1,4-cyclohexanediamine	c-1,4- DACH	: NH ₂ NH ₂	8.1×10^{2}	3.71
<i>p</i> -phenylenediamine	PPD	H_2N \longrightarrow NH_2	3.6	5.01
4-(1,3-dimethyl-2,3-dihydro-1H-benzoimidazol-2-yl)phenyl)dimethylamine	N-DMBI	N: N:	3.9	2.97
1,8-diazabicyclo(5.4.0)undec- 7-ene	DBU	N.	7.5×10^7	18.7
3-(azepan-1-yl)propan-1- amine	APA	N NH_2	3.9×10^{4}	6.36
3-(azepan-1-yl)- <i>N</i> -methylpropan-1-amine	AMPA	Ü, H	1.9×10^{1}	3.81

^aFor each dedopant, the full name, acronym, and the structural formula are given.

consumption with low cost and commercial availability, but for that the polymer has to be transformed into its neutral (undoped) state.

Efforts to make neutral (undoped) PEDOT:PSS have been made using aliphatic amines such as polyethylenimine (PEI),

diethylenetriamine (DETA), and 1,8-diazabicyclo[5.4.0]-undec-7-ene (DBU) (structures shown in Table 1 and Table S1) for a variety of applications such as PEDOT batteries, neuromorphic devices, field-effect transistors, and low-work function electrodes.¹¹⁻¹⁵ Other applications of dedoped

PEDOT:PSS have been reported in organic solar cells, ¹⁶ polymer-based thermoelectric devices, ^{17–19} and electrochromic devices, ²⁰ highlighting the potential of dedoped PEDOT:PSS in a broad range of applications. However, the exact mechanism of chemical dedoping is poorly understood, preventing the rational design of molecules that can optimize novel device fabrication procedures in various fields. For neutral PEDOT:PSS specifically, it would be highly valuable to develop a method that is more controllable and faster than the commonly used vapor deposition of PEI. ^{14,15} Additionally, understanding the mechanism of dedoping is an essential first step in unlocking routes to air-stable devices with neutral PEDOT:PSS. Currently, neutral PEDOT:PSS films are not stable as PEDOT reoxidizes in air, ^{21,22} which is exploited in air/PEDOT-battery devices. ^{11–13} Recent efforts show that this phenomenon can be partially prevented by encapsulation in a nitrogen atmosphere. ²³

Previously reported strong dedopants for PEDOT:PSS (PEI, DETA, and DBU) are aliphatic amines that act both as a reducing agent and as a Brønsted–Lowry base. However, other aliphatic amines such as triethylamine (TEA) were reported to dedope PEDOT:PSS only mildly. Amines can reduce oxidized PEDOT chain segments by a single electron transfer (SET) reaction but can also engage in abstracting a proton from PSSH to form an ammonium ion, which is unable to act as a reducing agent. The largely different dedoping strengths of DETA and TEA indicate that the dedoping mechanism comprises more than a straightforward SET reaction from an amine.

To investigate the structural motif that endows compounds like PEI, DETA, and DBU with a strong tendency to dedope PEDOT:PSS and elucidate the mechanism of the dedoping process, we investigate the functional groups in amines that create conditions for strong dedoping. The results of these experiments are then used to postulate a reaction mechanism. We support this mechanism by synthesizing two derivatives of DBU and comparing their dedoping capacity to predictions based on the proposed reaction pathway. Finally, we select an aliphatic amine that forms a stable aqueous dispersion with PEDOT:PSS and that strongly dedopes PEDOT:PSS upon heating a film cast from the two components. This allows creating charge-neutral, undoped PEDOT:PSS films in a simple one-step process.

METHODS

Sample Preparation. Borosilicate glass substrates (3 cm × 3 cm) were cleaned by rinsing with acetone, rubbing with an isopropanol drenched cloth, and rinsing with isopropanol before depositing gold (50 nm) on chromium (5 nm) electrodes by thermal evaporation in high vacuum (\sim 3 \times 10⁻⁷ mbar). The electrode width was either 4 or 6 mm, and the corresponding shortest electrode-to-electrode distance was 9.5 or 6.3 mm, respectively, depending on the layout used. The substrates with Cr/Au electrodes were cleaned by 30 min UV/ O₃ treatment (UVP PR-100). An aqueous dispersion of highly conductive PEDOT:PSS (Clevios PH1000, Heraeus) containing 3-5 vol % ethylene glycol (Sigma-Aldrich, 99.8%) was filtered through a 0.45 µm filter (Pall Life Sciences, Acrodisc, PVDF membrane) and then spin-coated at either 1000 or 2400 rpm for 60 s, resulting in films of ~100 and ~55 nm, respectively. The PEDOT:PSS layer was annealed at 120 °C for a minimum of 2 min in an ambient atmosphere. Dedopants listed in Table 1 and Table S1 (Supporting Information) were

obtained from commercial suppliers and used as received. Details on suppliers and purity are provided in Table S2. For dedoping, the PEDOT:PSS layer was fully covered by dropcasting the dedopant and then heated on a hot plate in an ambient atmosphere (unless stated otherwise) to facilitate the dedoping reaction and evaporate excess dedopant. For dedopants solid at room temperature, the dedopant was drop-cast on top of the PEDOT:PSS film from a saturated solution in isopropanol. The conductivity of the layer was probed during heating of the layer. UV-vis-NIR absorption spectra were recorded before and after dedoping. The R_O and $R_{\rm E}$ of PPD and N-DMBI and the $R_{\rm E}$ of TeMEDA were measured on PEDOT:PSS layers spin-coated at 2400 rpm. All other $R_{\rm E}$ and $R_{\rm O}$ values were determined for PEDOT:PSS layers spin-coated at 1000 rpm. The lowest attained conductivities and the temperatures at which these conductivities are reached are collected in Table S1.

For preparing a dedoped (neutral) PEDOT:PSS film from solution directly, the initial solution contained a volume percentage of DEMTA and additional base as indicated. For spin-coating the same procedure as above was used to form the layer of PEDOT:PSS. The conductivity and absorbance of the PEDOT:PSS layer were assessed after annealing at 120 °C.

Characterization. Two-point probe current-voltage (I-V) measurements were performed using an Agilent 4155C semiconductor analyzer. Absorption spectra were measured by using a PerkinElmer Lambda 900 or a Lambda 1050 spectrometer. Cyclic voltammetry measurements were performed inside a nitrogen-filled glovebox using an Autolab PGSTAT30 potentiostat. A 0.1 M solution of tetrabutylammonium hexafluorophosphate in dichloromethane was used as the electrolyte. Potentials are reported versus Ag/AgCl. ¹H NMR (400 MHz) and ¹³C NMR (100 MHz) spectra were recorded on a Varian Mercury spectrometer. Chemical shifts are given in ppm and referenced to the deuterated solvent residual peak. Matrix-assisted laser desorption ionization timeof-flight (MALDI-TOF) mass spectroscopy was recorded on a Bruker Autoflex Speed spectrometer by using α -cyano-4hydroxycinnamic (CHCA) acid as matrix.

Synthesis. Reagents used as starting materials and commercial solvents were used as received without any further purification.

3-(Azepan-1-yl)propan-1-amine (APA). 1,8-Diazabicyclo-[5.4.0]undec-7-ene (6.5 g, 42.7 mmol) was dissolved in ethanol (80 mL) under argon at 0 °C. Glacial acetic acid (2.5 mL) was added, followed by sodium borohydride (1.62 g, 42.8 mmol, 1.0 equiv) under vivid stirring. The mixture was concentrated under reduced pressure and redissolved in ethyl acetate (80 mL) and water (10 mL). Sufficient Na₂SO₄ was added to fully absorb the water. The suspension was filtered, and the filtrate was concentrated under reduced pressure to afford APA as a colorless oil (3.06 g, 19.6 mmol, 46%). ¹H NMR (400 MHz, CDCl₃): δ 2.73 (2H, t, J = 6.8 Hz, H₂N- CH_2), 2.61 (4H, t, J = 5.4 Hz, $-N-CH_2-$), 2.51 (2H, t, J =7.3 Hz, $-N-CH_2-CH_2-CH_2-NH_2$), 1.55–1.71 (10H, m). ¹³C NMR (100 MHz, CDCl₃): δ 56.06, 55.59, 40.80, 31.39, 28.00, 26.91. MALDI-TOF-MS (CHCA): calculated m/z156.16; found m/z 153.30, 157.33 ([M + H]⁺).

3-(Azepan-1-yl)-N-methylpropan-1-amine (AMPA). 1,8-Diazabicyclo[5.4.0]undec-7-ene (6.5 g, 42.7 mmol) was dissolved in benzene (75 mL) under argon. Methyl iodide (3.72 mL, 59.8 mmol, 1.4 equiv) was added gradually, and the mixture was stirred at room temperature for 30 min. The

mixture was concentrated under reduced pressure when a white solid precipitated which was readily redissolved upon the addition of ethanol (80 mL) under argon. Sodium borohydride (1.62 g, 42.8 mmol, 1.0 equiv) was added portionwise, and the mixture was stirred at room temperature for 2 h. The ethanol was evaporated under reduced pressure, and the concentrate was redissolved in ethyl acetate (80 mL) and water (10 mL). Sufficient Na₂SO₄ was added to fully absorb the water. The suspension was filtered, and the filtrate was concentrated under reduced pressure to afford the desired product as a light-vellow oil (6.0 g, 35.2 mmol, 82%). ¹H NMR (400 MHz, CDCl₃): δ 2.70 (2H, t, I = 6.8 Hz, $HN-CH_2$), 2.66 (4H, t, I = 5.8 Hz, $-N-CH_2-$), 2.58 (2H, t, J = 7.0 Hz, $-N-CH_2-CH_2-CH_2-$ NH-CH₃), 2.46 (3H, s, N-CH₃), 1.71 (2H, p, I = 6.9 Hz, $N-CH_2-CH_2-CH_2-N$), 1.65 (4H, m), 1.60 (4H, m). ¹³C NMR (100 MHz, CDCl₃): δ 56.73, 55.57, 50.82, 36.13, 27.82, 27.01, 26.86. MALDI-TOF-MS (CHCA): calculated m/z170.18; found m/z 167.29, 171.32 ([M + H]⁺).

RESULTS AND DISCUSSION

We systematically investigated a range of relevant amines (Table 1) for their capacity to dedope PEDOT:PSS thin films. For dedoping, spin-coated PEDOT:PSS layers were fully covered by drop-casting the amine and subsequently heated on a hot plate. To quantify the dedoping capability, the electrical conductivity and the UV-vis-NIR absorption spectrum of the films were measured before and after applying the dedopant to provide two independent indicators for the resulting dedoping level. Apart from a decrease in conductivity, the transition from doped to neutral PEDOT:PSS is indicated by a decrease of the bipolaron absorption at wavelengths in the 1500-2500 nm range, 24,25 accompanied by a distinct rise of a polaron transition at 800-1000 nm. Further dedoping results in an increase of the absorption band around 650 nm of neutral PEDOT chains and a decrease in absorption of the polaron band. These changes in conductivity and absorption spectra are sensitive indicators of the dedoping level of PEDOT.

To quantify the dedoping efficacy, we define two figures of merit that describe the relative decrease in electrical conductivity (σ) measured at 1 V bias ($R_{\rm E}$) and the relative loss of absorbance (A) of the bipolaron band at 2500 nm compared to neutral absorption band at 650 nm ($R_{\rm O}$) in dedoped films.

$$R_{\rm E} = \frac{\sigma_{\rm pristine}}{\sigma_{\rm dedoped}} = \left(\frac{I_{\rm pristine}}{I_{\rm dedoped}}\right)_{V=1} \tag{1}$$

$$R_{\rm O} = \frac{[A(2500)/A(650)]_{\rm pristine}}{[A(2500)/A(650)]_{\rm dedoped}}$$
(2)

Under identical conditions and for constant film thickness, the figures of merit $R_{\rm E}$ and $R_{\rm O}$ as defined in eqs 1 and 2 are material properties. The $R_{\rm E}$ and $R_{\rm O}$ values were determined for a wide range of aliphatic amines with varied chemical structure (summarized in Table 1 and Figure 1). We note that the two figures of merit are not necessarily correlated which may be a result of structural changes to the film after dedoping. Extended versions of Table 1 and Figure 1 can be found in the Table S1 and Figure S1.

As characteristic examples of the dedoping efficacy of PEDOT:PSS by amines, we consider the effects of *N*-(2-aminoethyl)-1,2-ethanediamine (DEMTA) and *N,N,N',N'*-

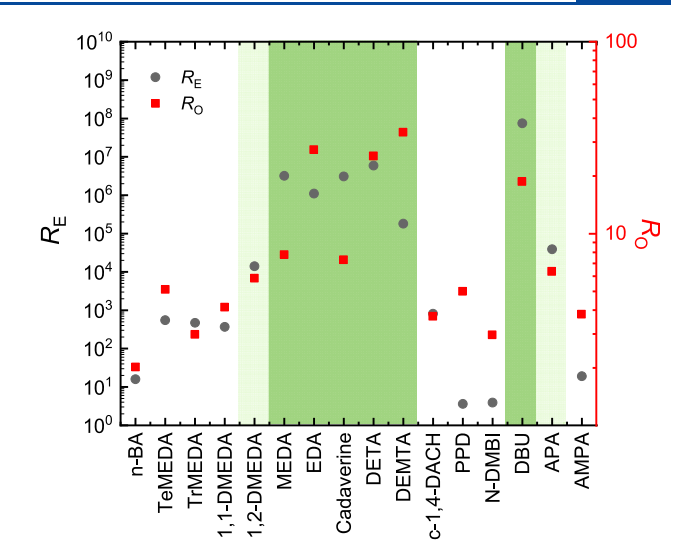


Figure 1. Correlation between $R_{\rm E}$ and $R_{\rm O}$ for dedoping PEDOT:PSS for the organic amines tested. Mild and strong dedopants are colored light green and dark green, respectively.

tetramethyl-1,2-ethanediamine (TeMEDA). The currentvoltage (I-V) characteristics reveal that the current, and thus conductivity, drops over 5 orders of magnitude for dedoping with DEMTA (Figure 2a), while only a decrease by 2 orders of magnitude occurs for TeMEDA (Figure 2c). To reach the lowest attainable conductivity, thermal annealing is required, suggesting that the dedoping is thermally activated. The UV-vis-NIR absorption spectra confirm the more effective dedoping by DEMTA (Figure 2b) compared to TeMEDA (Figure 2d). For the DEMTA-treated PEDOT:PSS film the bipolaron absorption at 1500-2500 nm virtually vanishes and is replaced by the strong absorption of neutral PEDOT around 650 nm. In contrast, the absorption spectrum of PEDOT:PSS recorded after dedoping with TeMEDA shows a combination of the bipolaron, polaron, and neutral absorption bands, indicating that dedoping is not complete.

To determine the influence of oxygen, we tested the dedoping by 1,2-ethanediamine (EDA) in ambient air and in N_2 atmosphere (<1 ppm of O_2 , <1 ppm of H_2O) (Figure S2). In an inert atmosphere the dedoping capacity is slightly higher, which agrees with a previous work.²⁶

Following the notion that DEMTA (Figure 2a,b) and DETA¹⁵ are capable of strongly dedoping PEDOT:PSS, while TeMEDA (Figure 2c,d) is not, we investigated which minimal combination of functionalities is essential for strong dedoping. The results suggest that the primary amine functional groups on DEMTA play an important role. To analyze the importance of primary amines, we tested the dedoping efficacy of PEDOT:PSS by *n*-butylamine (*n*-BA) and 1,2-ethanediamine (EDA). Figure 1 and Table 1 show that strong dedoping was achieved by using EDA but that *n*-BA is not an effective dedopant. Together with poor dedoping by TeMEDA, these results indicate that primary amines exert a crucial effect on the dedoping, but only when accompanied by a second amine group in the molecule.

Knowing that EDA is a strong dedopant for PEDOT:PSS while TeMEDA is not, we systematically investigated the dedoping capacity of all methyl-substituted EDA analogues to understand the influence of methyl substitution. The dedoping strength of *N*,*N*,*N*′-trimethyl-1,2-ethanediamine (TrMEDA), *N*,*N*-dimethyl-1,2-ethanediamine (1,1-DMEDA), *N*,*N*′-di-

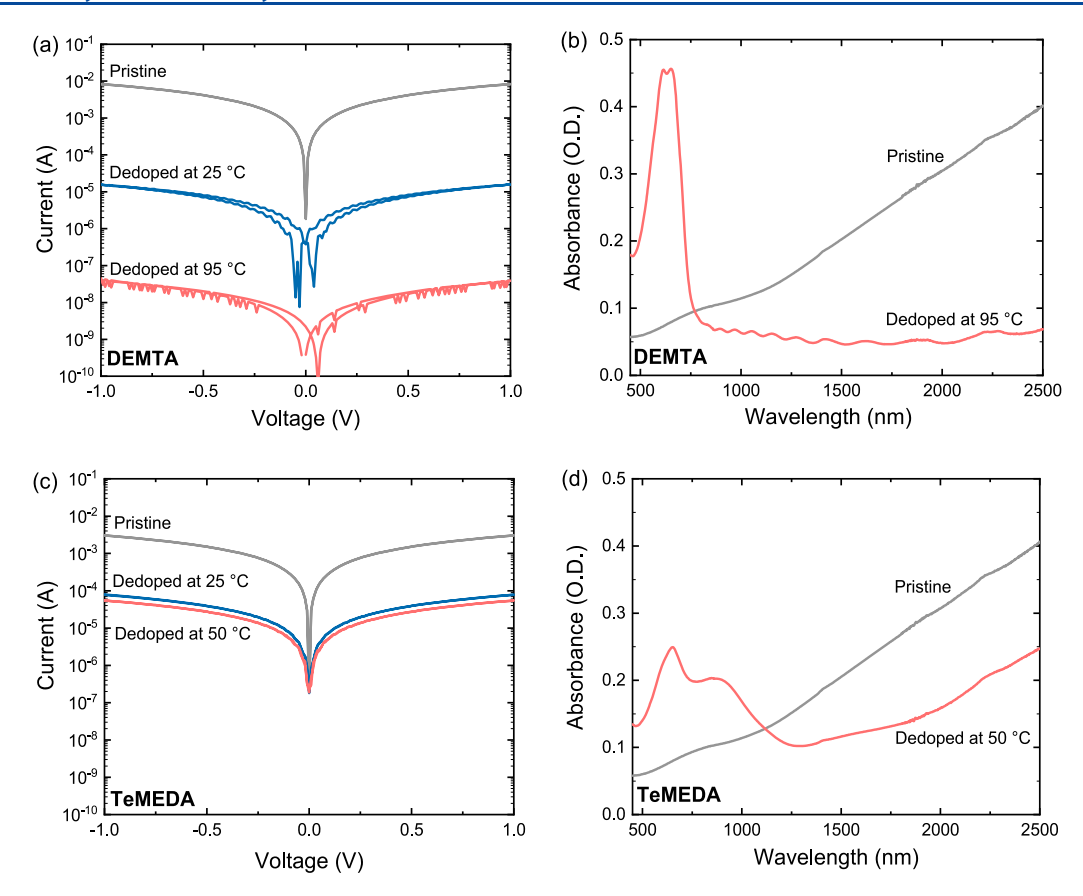


Figure 2. (a, c) Semilogarithmic I-V characteristics and (b, d) UV-vis-NIR spectra of pristine and dedoped PEDOT:PSS layers by using DEMTA (a, b) or TeMEDA (c, d) as dedopants. The PEDOT:PSS layer thickness was ~ 100 nm in (a, b, d) and ~ 55 nm in (c).

methyl-1,2-ethanediamine (1,2-DMEDA), and N-methyl-1,2-ethanediamine (MEDA) were assessed (Table 1 and Figure 1). Interestingly, both TrMEDA and 1,1-DMEDA do not dedope PEDOT:PSS strongly, while 1,2-DMEDA showed moderate dedoping capacity. MEDA, on the other hand, showed strong dedoping similar to EDA. From this we conclude that for effective dedoping toward neutral PEDOT:PSS a diamine is required of which neither amine group is tertiary. If one of the two amine groups is primary, the dedoping capacity is enhanced. Interestingly, these results contradict the trend in oxidation potential, as measured by cyclic voltammetry (Figure S3 and Table S3), which suggests a more intricate mechanism than single electron transfer and signifies the formation of another reducing species.

The difference in dedoping capacity between EDA and *n*-BA hints at an intramolecular reaction of two amine groups playing a role in the mechanism. To support this suggestion, we assessed the dedoping strength of three diamines with different spacer moieties, namely 1,5-pentanediamine (cadaverine), *p*-phenylenediamine (PPD), and *cis*-1,4-cyclohexanediamine (c-1,4-DACH). Their *R*_E and *R*_O values (Table 1 and Figure 1) indicate that the spacer should be sufficiently flexible to achieve dedoping. Both PPD and c-1,4-DACH dedope PEDOT:PSS only slightly, while cadaverine proved to be a strong dedopant. This conclusion, combined with the fact that *n*-BA does not strongly dedope PEDOT:PSS, firmly suggests that an intramolecular reaction takes place in which two amine groups need to be able to reach each other to effectively engage in dedoping of PEDOT:PSS.

In one-electron oxidation reactions of aliphatic amines, the amine radical cation formed is known to deprotonate at the α carbon, followed by oxidation of the α -amino radical to an iminium ion. 27-30 On the basis of this general mechanism and the electron-donating reactions of 4-(1,3-dimethyl-2,3-dihydro-1H-benzoimidazol-2-yl)phenyl)dimethylamine (N-DMBI),^{31,32} we formulated a tentative mechanism (Figure 3) that enables rationalizing the remarkable difference in dedoping capacities of the aliphatic amines tested. Figure 3 describes a possible sequence of steps for EDA as an example. The chain of reactions starts with the single electron transfer from the diamine (step 1). DFT calculations have shown that this is possibly followed by an intermediate 1,2-hydrogen shift (step 2)³³ and subsequent deprotonation (step 3) leading to an α -amino radical. The deprotonation is facilitated by the excess of base present. The outcome of steps 2 and 3 is identical to a direct deprotonation at the α -carbon atom followed by an electron transfer from the α -carbon to nitrogen. The α -amino radical then undergoes a second SET (step 4) to the iminium ion. $^{27-30}$ This iminium ion can instigate an intramolecular ring closure by reacting with the second amine group (step 5). We speculate that the product of step 5, which has similarities to the reactive functionality of N-DMBI, will then undergo another SET, 1,2-hydrogen shift, deprotonation, and a subsequent SET (steps 6-9). 27-32 The sum of reaction steps 6-9 can be viewed as a hydride extraction, as commonly assumed for N-DMBI.

For EDA it is likely that the reaction product of reaction step 9 will undergo deprotonation (step 10) to form aziridin-2-imine. The formed N=C-N moiety is structurally similar to

Figure 3. Proposed reaction mechanism (steps 1-11) of diamine oxidation for EDA as an example.

the same motif in DBU and is thus likely to undergo another electron transfer reaction (step 11), as described in the literature on the electron-donating properties of DBU. 13,34,35 The complete reaction mechanism then includes reaction steps 10 and 11 (Figure 3). The importance of reaction step 11 is demonstrated by the dedoping strength of N-DMBI and DBU. Intriguingly, it was found that N-DMBI does not dedope PEDOT:PSS strongly, even though it follows reaction steps 6–9, while DBU does, following reaction step 11. It can thus be concluded that reaction step 11 is crucial for effective dedoping and that reaction step 9 is not the likely end point of the mechanism. The mechanism comprises four deprotonations, which is facilitated by the excess of amines.

Despite that the mechanism hypothesized in Figure 3 is speculative and the intermediates have not been identified, it enables the rationalizing of the remarkable differences in dedoping strength of the methyl-substituted 1,2-ethanediamines. To illustrate this, Figure 4 shows the expected intermediate reaction products from step 9 for EDA (1), MEDA (2), 1,2-DMEDA (3), 1,1-DMEDA (4), and TrMEDA (5) and the product of step 4 for TeMEDA (6). The expected subsequent reactions are then indicated. It is apparent that compounds 5 and 6 cannot reach reaction step 11. Compound 4 can only undergo deprotonation (step 10) to form N_iN_j dimethyl-2H-azirin-3-amine with a highly strained doublebond ring structure. On the other hand, compounds 1, 2, and 3 form aziridinimine or its methyl-substituted derivatives. We note that ((E)-N-(1-methylaziridin-2-ylidene)methanamine)(from 3) corresponds to a known compound.³⁶ The degree to which the intermediates can progress in this reaction mechanism correlates to their dedoping strength. Correspondingly, compounds 4, 5, and 6 do not dedope PEDOT:PSS, while 1, 2, and 3 dedope PEDOT:PSS mildly or even strongly. The remarkable dedoping capacity of 3, being stronger than that of 4, 5, and 6 but lower than 1 and 2, can possibly be explained by the fact that the product of reaction step 11 is not stabilized by a hydride shift, while it is for 2 and 1. Here it

should be noted that DBU also does not benefit from this hydride shift after single electron transfer. We note, however, that PEDOT:PSS is almost fully dedoped by DBU due to the large excess employed in drop-casting.

To further support the proposed mechanism, we synthesized and compared the dedoping capacity of 3-(azepan-1-yl)propan-1-amine (APA) and 3-(azepan-1-yl)-N-methylpropan-1-amine (AMPA) (Figure 5). Following the proposed mechanism, APA should dedope PEDOT:PSS in a similar fashion as 1,2-DMEDA, while AMPA should only induce very weak dedoping comparable to TrMEDA. The reaction sequences for both compounds are detailed in Figures S4 and S5. At first glance it might seem like APA would have similar dedoping strength as 1,1-DMEDA because of the tertiary-primary diamine functionality. However, where reaction 10 is hindered for 1,1-DMEDA because of ring strain, this reaction is not hindered for APA. Therefore, DBU can be formed from APA after reaction step 10 (Figure 5). Even though DBU can be formed, the dedoping strength is expected to be less than that reported for DBU as the formed concentration of DBU is much lower compared to pure DBU. Therefore, the predicted dedoping strength is mild, much akin to 1,2-DMEDA. For AMPA, reaction 10 cannot occur as no amine-bound hydrogens remain after reaction 9, similar to TrMEDA (Figure 5). The proposed reaction products following reactions 1-9 are displayed in Figure 5.

To test the validity of our mechanism and the predicted dedoping strength of APA and AMPA, conductivity and absorption experiments were conducted on PEDOT:PSS, covered by both compounds through drop-casting. As the mechanism predicted, AMPA dedopes PEDOT:PSS weakly, showing a minimal decrease in conductivity (Figure 6a) and a slight increase in intensity of the absorption peak attributed to neutral PEDOT:PSS (Figure 6b). In contrast, APA shows a substantial dedoping indicated by a more than 4 orders of magnitude decrease in conductivity (Figure 6c) and a pronounced presence of neutral PEDOT:PSS in the absorption

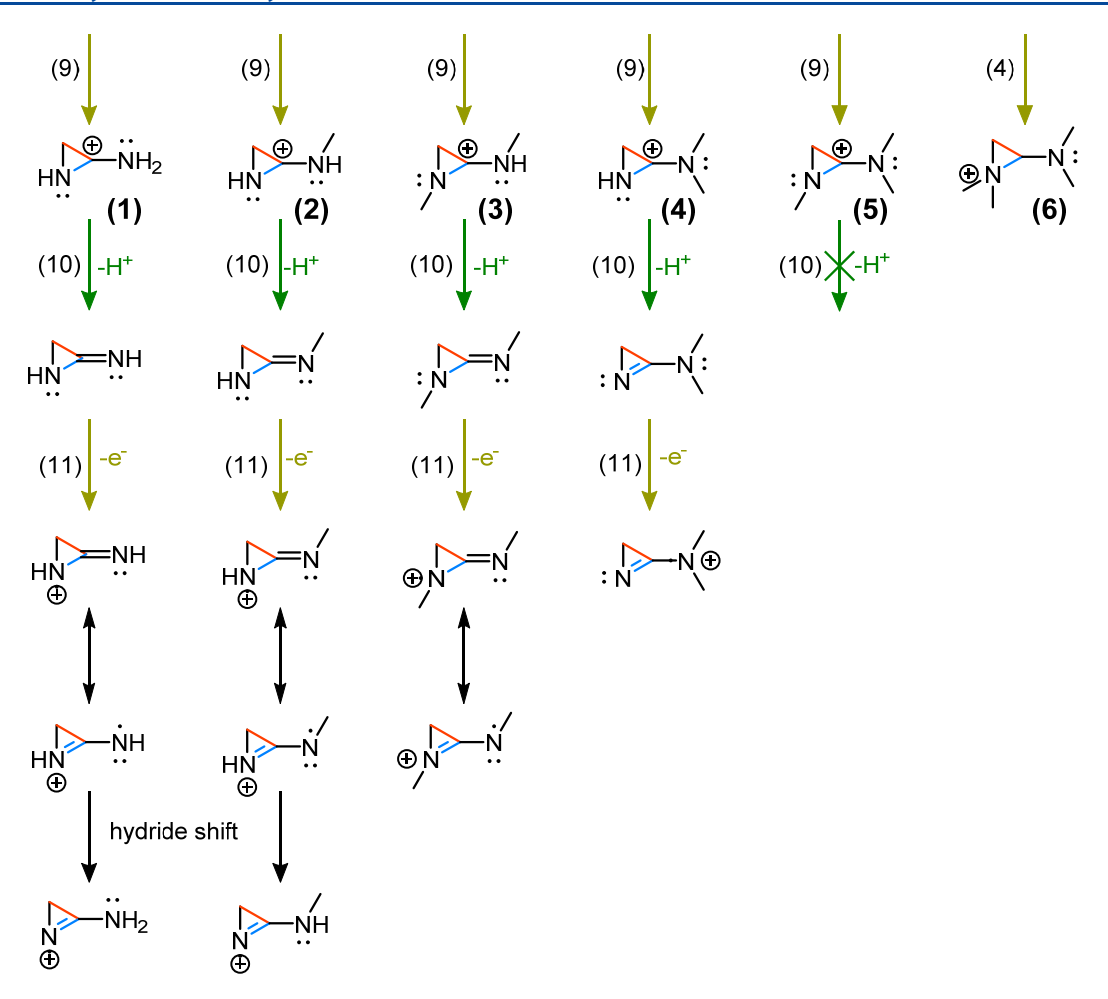


Figure 4. End of the cascade of reactions according to the mechanism of Figure 3 for the compounds EDA (1), MEDA (2), 1,2-DMEDA (3), 1,1-DMEDA (4), TrMEDA (5), and TeMEDA (6). For EDA and MEDA, the hydride-shift-induced stabilization is also depicted.

spectrum (Figure 6d). The decrease in conductivity and change in absorption spectra for dedoping with APA is very similar to that of 1,2-DMEDA.

Utilizing the insights in the proposed dedoping mechanism, we formulated a PEDOT:PSS dispersion with a dedopant added in solution that after spin-coating results in films that can be converted into neutral PEDOT:PSS when heated. This solution dedoping recipe enables a straightforward method for fabricating neutral PEDOT:PSS layers from a single casting step. The formulation contains the aqueous PEDOT:PSS dispersion, ethylene glycol, and DEMTA in a 0.63:0.03:0.33 (v/v/v) ratio. Ethylene glycol improves the morphology of PEDOT:PSS, 37-39 while DEMTA was selected because of its sufficiently high activation temperature (95 °C) for dedoping. We note that flocculation occurs if PEDOT:PSS is strongly dedoped in solution. Using the PEDOT:PSS/DEMTA dispersions, films were spin-coated on a glass substrate and heated to 120 °C. The resulting films exhibit very low conductivity (Figure 7a), and the UV-vis-NIR absorption spectra confirm strong dedoping (Figure 7b). Hence, neutral PEDOT:PSS films were fabricated in a one-step process from a single solution and subsequent thermal annealing, greatly enhancing ease of fabrication. Note that conductivity and absorption measurements of a pristine film with analogue morphology and layer thickness cannot be obtained for this fabrication method.

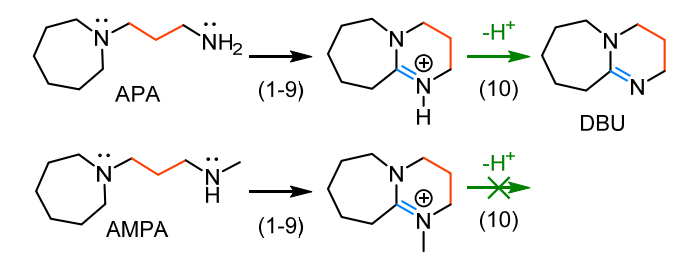


Figure 5. Structural formulas of the proposed reaction products of APA and AMPA after reaction steps 10 and 9, respectively.

The formulation of the PEDOT:PSS-DEMTA solution can be tailored to a specific application, and lower levels of dedoping can be obtained by decreasing the volume percentage of DEMTA (Figure S6). Even for the illustrative example of 5 vol %, DEMTA is in excess of PEDOT:PSS (solid content maximum 1.3 wt % in PH1000 dispersion), and the decrease in dedoping at 5 vol % is therefore attributed to the relatively lower pH of the 5 vol % solution compared to 33 vol %. This influence of pH on dedoping was later confirmed after increasing the pH of a PEDOT:PSS-DEMTA 5 vol % solution by adding NaOH and obtaining stronger dedoped layers in the process (Figure S7). The pH dependence is consistent with the proposed mechanism that involves four deprotonation steps.

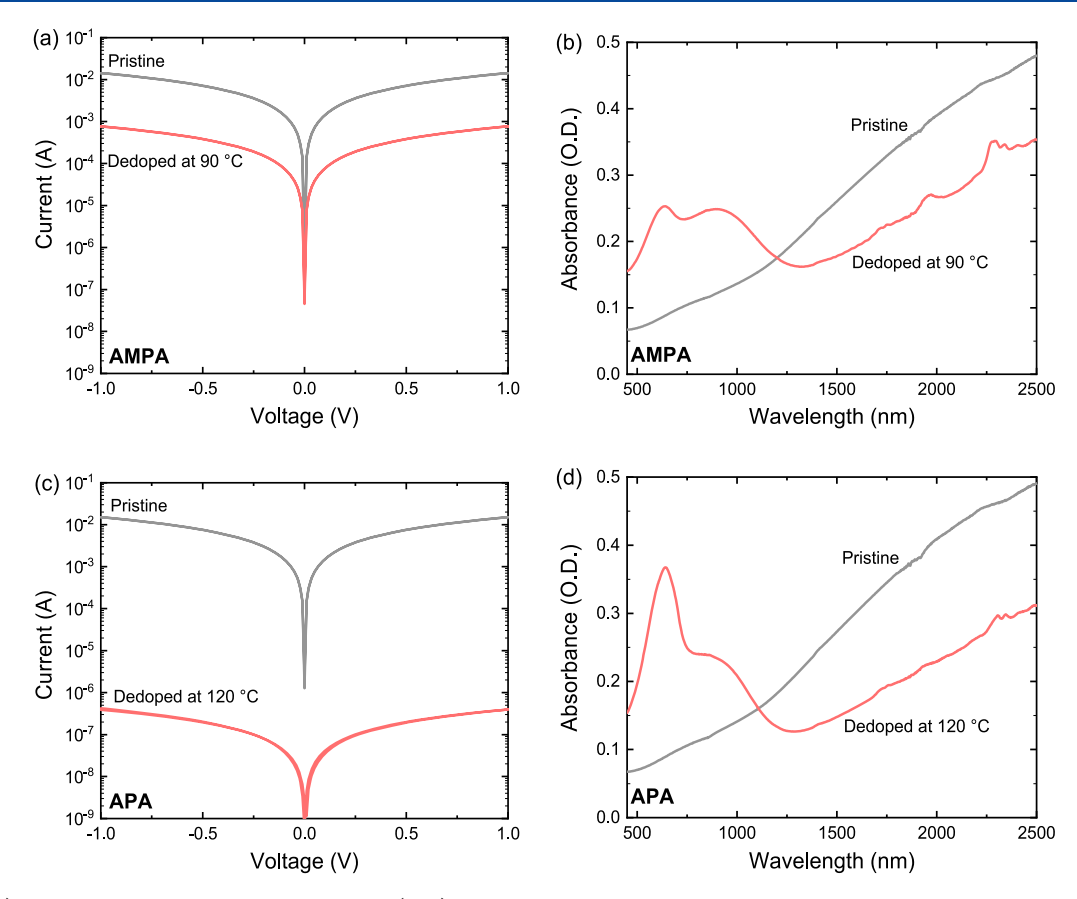


Figure 6. (a, c) Semilogarithmic I-V characteristics and (b, d) UV-vis-NIR spectra of pristine and dedoped PEDOT:PSS layers by using AMPA (a, b) or APA (c, d) as dedopants. The PEDOT:PSS layer thickness was ~ 100 nm.

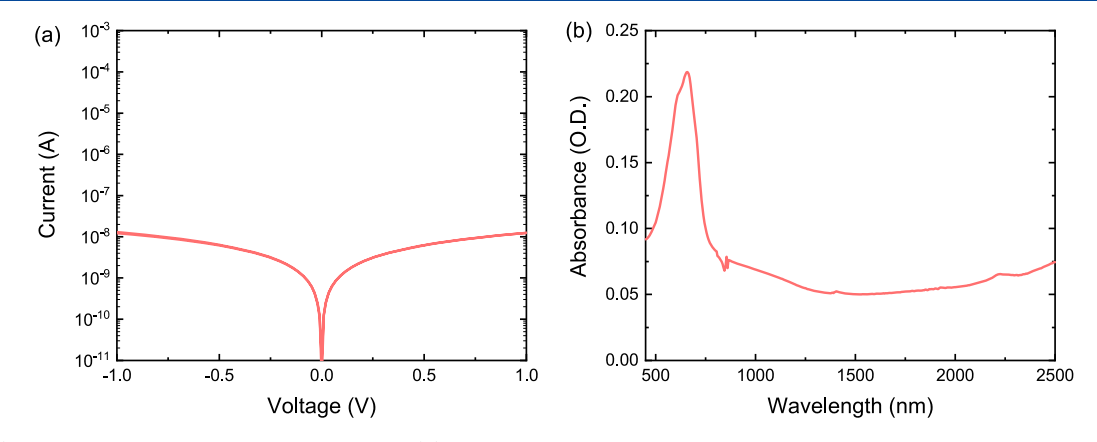


Figure 7. (a) Semilogarithmic I-V characteristics and (b) UV-vis-NIR absorption spectrum for a PEDOT:PSS layer spin-coated from a dispersion of aqueous PEDOT:PSS/EG/DEMTA (0.63:0.03:0.33 (v/v/v)).

CONCLUSION

By systematically investigating the dedoping efficacy for a range of aliphatic amines, we have identified the presence of at least two primary or secondary amines that can participate in an intramolecular reaction as the principal structural motif that is required in organic aliphatic amines to strongly dedope PEDOT:PSS films. On the basis of this structural motif, we propose a multistep reaction mechanism that involves sequential electron transfer and deprotonation steps. In the proposed mechanism the aliphatic amines act as both an electron donor and proton acceptor. The proposed mechanism identifies an N=C-N moiety formed in an intramolecular reaction as the structural element that is crucial to the achieved

strong dedoping. All experimental observations are qualitatively consistent with the mechanism, and its predictive value was demonstrated by synthesizing two aliphatic diamine derivatives (AMPA and APA) and comparing their dedoping efficacy.

The proposed mechanism is complex, and we have not been able to identify intermediate products. Despite its tentative nature, the mechanism contributes to our understanding of the reductive capability of aliphatic amines. It also rationalizes the remarkable difference in dedoping efficacy of several aliphatic amines and provides a guideline to further optimize methods in fabricating dedoped PEDOT:PSS films.

Using the obtained insights in the dedoping mechanism, we developed a new formulation of the aqueous dispersion of PEDOT:PSS in which ethylene glycol and DEMTA are added, and that allows to spin-coat PEDOT:PSS films that can be converted into a strongly dedoped film by heating to 120 °C. By casting the PEDOT:PSS with the dedopant from solution in a single step, we expect that neutral PEDOT:PSS can be fabricated with classic roll-to-roll printing techniques. Additionally, the thermal activation of dedoping enables infrared photopatterning. These fabrication methods open the pathway to rapidly producing mixed ion—electron organic (semi)-conductors with all commercially available ingredients.

ASSOCIATED CONTENT

S Supporting Information

The Supporting Information is available free of charge on the ACS Publications website at DOI: 10.1021/acs.jpcc.9b07718.

Extended versions of Table 1 and Figure 1 with data for more amines; cyclic voltammetry data of selected amines; electrical conductivity and UV-vis-NIR absorption spectra of several control experiments (effect of inert atmosphere, effect of base) (PDF)

AUTHOR INFORMATION

Corresponding Authors

*E-mail y.b.v.d.burgt@tue.nl.

*E-mail r.a.j.janssen@tue.nl.

ORCID

Scott T. Keene: 0000-0002-6635-670X Stefan C. J. Meskers: 0000-0001-9236-591X Yoeri van de Burgt: 0000-0003-3472-0148 René A. J. Janssen: 0000-0002-1920-5124

Notes

The authors declare no competing financial interest.

ACKNOWLEDGMENTS

We acknowledge funding from the Ministry of Education, Culture and Science (Gravity program 024.001.035), the European Research Council under the European Union's Seventh Framework Programme (FP/2007-2013)/ERC Grant Agreement No. 339031, and European Union's Horizon 2020 Research and Innovation Programme, grant agreement No. 802615, and the NWO Spinoza prize awarded to R.A.J.J. by The Netherlands Organization for Scientific Research (NWO). A.S. and S.T.K. acknowledge financial support from the National Science Foundation and the Semiconductor Research Corporation, E2CDA Award #1739795. Additionally, S.T.K. acknowledges the Stanford Graduate Fellowship fund for support.

■ REFERENCES

- (1) Jonas, F.; Schrader, L. Conductive modifications of polymers with polypyrroles and polythiophenes. *Synth. Met.* **1991**, *41*–*43*, 831–836.
- (2) Heywang, G.; Jonas, F. Poly(alkylenedioxythiophene)s new, very stable conducting polymers. *Adv. Mater.* **1992**, *4*, 116–118.
- (3) Elschner, A.; Kirchmeyer, S.; Lövenich, W.; Merker, U.; Reuter, K. PEDOT: Principles and Application of an Intrinsically Conductive Polymer; CRC Press: Boca Raton, FL, 2010.
- (4) Sun, K.; Zhang, S.; Li, P.; Xia, Y.; Zhang, X.; Du, D.; Isikgor, F. H.; Ouyang, J. Review on application of PEDOTs and PEDOT:PSS in

- energy conversion and storage devices. J. Mater. Sci.: Mater. Electron. 2015, 26, 4438-4462.
- (5) Shi, H.; Liu, C.; Jiang, Q.; Xu, J. Effective Approaches to improve the electrical conductivity of PEDOT:PSS: A review. *Adv. Electron. Mater.* **2015**, *1*, 1500017.
- (6) Zeglio, E.; Rutz, A. L.; Winkler, T. E.; Malliaras, G. G.; Herland, A. Conjugated polymers for assessing and controlling biological functions. *Adv. Mater.* **2019**, *31*, 1806712.
- (7) Khodagholy, D.; Doublet, T.; Quilichini, P.; Gurfinkel, M.; Leleux, P.; Ghestem, A.; Ismailova, E.; Herve, T.; Sanaur, S.; Bernard, C.; Malliaras, G. G. In vivo recordings of brain activity using organic transistors. *Nat. Commun.* **2013**, *4*, 1575.
- (8) Owens, R. M.; Malliaras, G. G. Organic electronics at the interface with biology. MRS Bull. 2010, 35, 449-456.
- (9) Rivnay, J.; Leleux, P.; Ferro, M.; Sessolo, M.; Williamson, A.; Koutsouras, D. A.; Khodagholy, D.; Ramuz, M.; Strakosas, X.; Owens, R. M.; et al. High-performance transistors for bioelectronics through tuning of channel thickness. *Sci. Adv.* **2015**, *1*, No. e1400251.
- (10) Giovannitti, A.; Maria, I. P.; Hanifi, D.; Donahue, M. J.; Bryant, D.; Barth, K. J.; Makdah, B. E.; Savva, A.; Moia, D.; Zetek, M.; Barnes, P. R.F.; Reid, O. G.; Inal, S.; Rumbles, G.; Malliaras, G. G.; Nelson, J.; Rivnay, J.; McCulloch, I. The role of the side chain on the performance of n-type conjugated polymers in aqueous electrolytes. *Chem. Mater.* **2018**, *30*, 2945—2953.
- (11) Xuan, Y.; Sandberg, M.; Berggren, M.; Crispin, X. An all-polymer-air PEDOT battery. *Org. Electron.* **2012**, *13*, 632–637.
- (12) Tehrani, Z.; Korochkina, T.; Govindarajan, S.; Thomas, D. J.; O'Mahony, J.; Kettle, J.; Claypole, T. C.; Gethin, D. T. Ultra-thin flexible screen printed rechargeable polymer battery for wearable electronic applications. *Org. Electron.* **2015**, *26*, 386–394.
- (13) Reyes-Reyes, M.; López-Sandoval, R. Optimizing the oxidation level of PEDOT anode in air-PEDOT battery. *Org. Electron.* **2018**, *52*, 364–370.
- (14) Van de Burgt, Y.; Lubberman, E.; Fuller, E. J.; Keene, S. T.; Faria, G. C.; Agarwal, S.; Marinella, M. J.; Talin, A. A.; Salleo, A. A non-volatile organic electrochemical device as a low-voltage artificial synapse for neuromorphic computing. *Nat. Mater.* **2017**, *16*, 414–418.
- (15) Fabiano, S.; Braun, S.; Liu, X.; Weverberghs, E.; Gerbaux, P.; Fahlman, M.; Berggren, M.; Crispin, X. Poly(ethylene imine) impurities induce n-doping reaction in organic (semi)conductors. *Adv. Mater.* **2014**, *26*, 6000–6006.
- (16) Li, Z.; Qin, F.; Liu, T.; Ge, R.; Meng, W.; Tong, J.; Xiong, S.; Zhou, Y. Optical properties and conductivity of PEDOT:PSS films treated by polyethylenimine solution for organic solar cells. *Org. Electron.* **2015**, *21*, 144–148.
- (17) Lee, S. H.; Park, H.; Son, W.; Choi, H. H.; Kim, J. H. Novel solution-processable, dedoped semiconductors for application in thermoelectric devices. *J. Mater. Chem. A* **2014**, *2*, 13380–13387.
- (18) Massonnet, N.; Carella, A.; Jaudouin, O.; Rannou, P.; Laval, G.; Celle, C.; Simonato, J.-P. Improvement of the Seebeck coefficient of PEDOT:PSS by chemical reduction combined with a novel method for its transfer using free-standing thin films. *J. Mater. Chem. C* **2014**, 2, 1278–1283.
- (19) Park, H.; Lee, S. H.; Kim, F. S.; Choi, H. H.; Cheong, I. W.; Kim, J. H. Enhanced thermoelectric properties of PEDOT:PSS nanofilms by a chemical dedoping process. *J. Mater. Chem. A* **2014**, *2*, 6532–6539.
- (20) Beaujuge, P. M.; Reynolds, J. R. Color Control in π -conjugated organic polymers for use in electrochromic devices. *Chem. Rev.* **2010**, 110, 268–320.
- (21) Singh, K.; Crispin, X.; Zozoulenko, I. V. Oxygen reduction reaction in conducting polymer PEDOT: Density functional theory study. *J. Phys. Chem. C* **2017**, *121*, 12270–12277.
- (22) Mitraka, E.; Jafari, M. J.; Vagin, M.; Liu, X.; Fahlman, M.; Ederth, T.; Berggren, M.; Jonsson, M. P.; Crispin, X. Oxygen-induced doping on reduced PEDOT. J. Mater. Chem. A 2017, 5, 4404–4412.

- (23) Keene, S. T.; Melianas, A.; van de Burgt, Y.; Salleo, A. Mechanisms for enhanced state retention and stability in redox-gated organic neuromorphic devices. *Adv. Electron. Mater.* **2019**, *5*, 1800686.
- (24) Sonmez, G.; Sonmez, H. B.; Shen, C. K. F.; Wudl, F. Red, green, and blue colors in polymeric electrochromics. *Adv. Mater.* **2004**, *16*, 1905–1908.
- (25) Sonmez, G.; Schottland, P.; Reynolds, J. R. PEDOT/PAMPS: An electrically conductive polymer composite with electrochromic and cation exchange properties. *Synth. Met.* **2005**, *155*, 130–137.
- (26) De Leeuw, D. M.; Simenon, M. M. J.; Brown, A. R.; Einerhand, R. E. F. Stability of n-type doped conducting polymers and consequences for polymeric microelectronic devices. *Synth. Met.* **1997**, 87, 53–59.
- (27) Mann, C. K.; Barnes, K. K. Electrochemical oxidation of primary aliphatic amines. *J. Org. Chem.* **1967**, 32, 1474–1479.
- (28) Smith, P. J.; Mann, C. K. Electrochemical dealkylation of aliphatic amines. J. Org. Chem. 1969, 34, 1821–1826.
- (29) Chow, Y. L.; Danen, W. C.; Nelsen, S. F.; Rosenblatt, D. H. Nonaromatic aminium radicals. *Chem. Rev.* **1978**, *78*, 243–274.
- (30) Zhang, X.; Yeh, S.-R.; Hong, S.; Freccero, M.; Albini, A.; Falvey, D. E.; Mariano, P. S. Dynamics of α-CH deprotonation and α-desilylation reactions of tertiary amine cation radicals. *J. Am. Chem. Soc.* **1994**, *116*, 4211–4220.
- (31) Wei, P.; Oh, J. H.; Dong, G.; Bao, Z. Use of a 1*H*-benzoimidazole derivative as an n-type dopant and to enable air-stable solution-processed n-channel organic thin-film transistors. *J. Am. Chem. Soc.* **2010**, *132*, 8852–8853.
- (32) Naab, B. D.; Guo, S.; Olthof, S.; Evans, E. G. B.; Wei, P.; Millhauser, G. L.; Kahn, A.; Barlow, S.; Marder, S. R.; Bao, Z. Mechanistic Study on the solution-phase n-doping of 1,3-dimethyl-2-aryl-2,3-dihydro-1*H*-benzoimidazole derivatives. *J. Am. Chem. Soc.* **2013**, *135*, 15018–15025.
- (33) Yates, B. F.; Radom, L. Intramolecular hydrogen migration in ionized amines: A theoretical study of the gas-phase analogues of the Hofmann-Lóffler and related rearrangements. *J. Am. Chem. Soc.* **1987**, 109, 2910–2915.
- (34) Hu, L.; Liu, T.; Duan, J.; Ma, X.; Ge, C.; Jiang, Y.; Qin, F.; Xiong, S.; Jiang, F.; Hu, B.; et al. An amidine-type n-dopant for solution-processed field-effect transistors and perovskite solar cells. *Adv. Funct. Mater.* **2017**, 27, 1703254.
- (35) Cruz-Cruz, I.; Reyes-Reyes, M.; Rosales-Gallegos, I. A.; Gorbatchev, A. Y.; Flores-Camacho, J. M.; López-Sandoval, R. Visible luminescence of dedoped DBU-treated PEDOT:PSS films. *J. Phys. Chem. C* **2015**, *119*, 19305–19311.
- (36) Quast, H.; Hergenröther, T. Photoextrusion von molekularem Stickstoff aus 5-Alkyliden-4,5-dihydro-1H-tetrazolen mit Vinyl- oder Phenyl-Substituenten. (E)-Aziridinimine und neuartige Produkte. *Chem. Ber.* **1992**, *125*, 2095–2101.
- (37) Lin, Y.-J.; Ni, W.-S.; Lee, J.-Y. Effect of incorporation of ethylene glycol into PEDOT:PSS on electron phonon coupling and conductivity. *J. Appl. Phys.* **2015**, *117*, 215501.
- (38) Rivnay, J.; Inal, S.; Collins, B. A.; Sessolo, M.; Stavrinidou, E.; Strakosas, X.; Tassone, C.; Delongchamp, D. M.; Malliaras, G. G. Structural control of mixed ionic and electronic transport in conducting polymers. *Nat. Commun.* **2016**, *7*, 11287.
- (39) Ouyang, J.; Xu, Q.; Chu, C. W.; Yang, Y.; Li, G.; Shinar, J. On the mechanism of conductivity enhancement in poly(3,4-ethylenedioxythiophene):poly(styrene sulfonate) film through solvent treatment. *Polymer* **2004**, *45*, 8443–8450.